Journal of Structural Biology xxx (xxxx) xxx–xxx

Contents lists available at ScienceDirect

Journal of Structural Biology

journal homepage: www.elsevier.com/locate/yjsbi

Copper ions trigger disassembly of neurokinin B functional amyloid and inhibit *de novo* assembly

Bhawantha M. Jayawardena[a], Mark R. Jones[a], Yuning Hong[b], Christopher E. Jones[a,*]

[a] School of Science and Health, Western Sydney University, Locked Bag 1797, Penrith, NSW, Australia
[b] Department of Chemistry and Physics, La Trobe Institute for Molecular Science, La Trobe University, Vic, Australia

ARTICLE INFO

Keywords:
Copper
Neuropeptide
Functional amyloid
neurokinin B
Tachykinin
Metal

ABSTRACT

The formation of amyloid is considered an intrinsic ability of most polypeptides. It is a structure adopted by many neuropeptides and neurohormones during the formation of dense core vesicles in secretory cells, yet the mechanisms mediating assembly and disassembly of these amyloids remain unclear. Neurokinin B is a neuropeptide thought to form an amyloid in secretory cells. It is known to coordinate copper, but the physiological significance of metal binding is not known. In this work we explored the amyloid formation of neurokinin B and the impact that metals had on the aggregation behaviour. We show that the production of neurokinin B amyloid is dependent on the phosphate concentration, the pH and the presence of a histidine at position 3 in the primary sequence. Copper(II) and nickel(II) coordination to the peptide, which requires the histidine imidazole group, completely inhibits amyloid formation, whereas zinc(II) slows, but does not inhibit fibrillogenesis. Furthermore, we show that copper(II) can rapidly disassemble preformed neurokinin B amyloid. This work identifies a role for copper in neurokinin B structure and reveals a mechanism for amyloid assembly and disassembly dependent on metal coordination.

1. Introduction

Amyloids are protein assemblies that have highly ordered, fibrillar, structures. These structures are usually composed of β-sheet-rich proteins where the β -strands are aligned perpendicular to the fibril axis, though fibrils containing helical proteins are known. (Knowles et al., 2014; Riek and Eisenberg, 2016; Tayeb-Fligelman et al., 2017) Amyloids are often considered in a negative light due to their role in disease, including neurodegenerative disorders such as Alzheimer's and Parkinson's disease, but it is now established that the amyloid fold may be an ancient structure that can be biologically useful. Termed 'functional amyloids', these structures are present in most domains of life including bacteria and humans. (Fowler et al., 2007) For instance, fibrillar Pmel17 promotes melanin synthesis in humans by accelerating the polymerization of melanin precursor molecules. (Fowler et al., 2006) A number of peptide hormones and neuropeptides are known to form functional amyloids in secretory vesicles. (Maji et al., 2009; Jacob et al., 2016)

A key unanswered question surrounding neuropeptide functional amyloids is how they disassemble once released from a secretory granule, since fibrils are notable for their structural stability and resistance to denaturants and proteases. (Knowles et al., 2014) One possibility is that dilution effects cause a functional amyloid to disassemble, and there is some support for this theory. (Maji et al., 2009) However, for neuropeptides released into the synaptic or peri-synaptic space dilution may not be great due to the limited synaptic volume and the fact that a high concentration of peptide is required to reach post-synaptic receptors. (Nassel, 2009; Nespovitaya et al., 2016) Recent evidence suggests that in the absence of dilution effects, the local environment can have a significant impact on not only the assembly but also the disassembly of fibrils, with pH and ionic strength conditions similar to the extracellular environment causing dissociation of functional amyloid of the neuropeptide β -endorphin. (Nespovitaya et al., 2016)

One neuropeptide identified as existing as an amyloid in pituitary secretory granules is the tachykinin, neurokinin B (NKB, neuromedin K). NKB is a key peptide for reproductive health but is, like many tachykinins, pleiotropic and involved in a diverse array of neurophysiological functions including neuroprotection and neuroinflammation. (Topaloglu et al., 2009) Amyloid formation by NKB has been predicted by computer simulations and shown experimentally *in vitro*, but there are no studies to date showing how it is disassembled into a form which can activate its G protein-coupled receptor. (Maji et al., 2009; Carballo-Pacheco et al., 2015) In a neuroprotective role, tachykinins, including

* Corresponding author.
E-mail address: c.jones@westernsydney.edu.au (C.E. Jones).

https://doi.org/10.1016/j.jsb.2019.09.011
Received 4 July 2019; Received in revised form 23 August 2019; Accepted 23 September 2019

NKB, appear to limit the toxicity associated with amyloid β (A β1-42) peptides and, for NKB, one mechanism that may account for this action is the apparent ability to co-assemble with A β (1–42) peptides to form heterogeneous fibrils that have reduced cytotoxicity compared to fibrils of A β (1–42). (Yankner et al., 1990; Flashner et al., 2011)

NKB has recently been identified as a metallopeptide, which can coordinate both copper(II) and nickel(II) via N-terminal amino acids. (Russino et al., 2013) *In vivo*, copper is the most relevant metal, but despite having a copper affinity that is sufficient to ensure NKB binds metal even in the presence of competing synaptic cuproproteins such as the prion protein (Shahzad et al., 2016), or gonadotropin releasing hormone (GnRH) (Gul et al., 2018), there is still no clear functional reason for it to bind copper. It appears copper-coordination does not modify the ability of NKB to activate its cognate G protein-coupled receptor NK3R, unlike the binding of copper to GnRH, nor does it appear to inhibit endocytosis of the NKB/NK3R complex. (Russino et al., 2013; Gajewska et al., 2016; Shahzad et al., 2016)

The coordination of metals can have substantial impact on the structure of proteins and peptides. This is particularly notable for metal-binding amyloidogenic proteins where, for instance, zinc(II) coordination to A β peptides accelerates fibrillogenesis but the binding of copper (II) appears to result in the formation of non-fibrillar aggregates. This suggests copper can divert A β (1-42) away from a fibrillar pathway. (House et al., 2009; Jiang et al., 2012; Mold et al., 2013) Further evidence suggests that copper binding results in amorphous aggregates even when added to fibrils of A β (1-42) or smaller A β peptides. (Dong et al., 2007; House et al., 2009) Similarly, copper appears to inhibit the prion fragment, PrP(106-126) from assembling into fibrils. (Kawahara et al., 2011) The ability of metals, particularly copper and zinc, to alter the fibrillary pathway led us to postulate that metals may adopt a similar role when binding to NKB. In this work we use a range of spectroscopic techniques *in vitro*, under conditions mimicking different physiological states, to investigate the effect of metals, primarily copper (II) and nickel(II) on the assembly and disassembly of NKB.

2. Materials and methods

Neurokinin B (NKB; DMHDFFVGLM-NH_2), neurokinin A (NKA; HKTDSFVGLM-NH_2), substance P (SP; RPKPQQFFGLM-NH_2) and NKB (H_3T) (DMTDFFVGLM-NH_2) were synthesised by Synpeptide (Shanghai, China) at a purity of > 95% and were used without further purification. Stock solutions were prepared in DMSO prior to dilution into required buffers. Peptide concentrations were estimated using the extinction coefficient of phenylalanine at 259 nm (190 M^{-1} cm^{-1}). Stock solutions of metal chlorides (Cu(II), Zn(II) and Ni(II), 50 mM) were prepared in metal-free MilliQ water (18 MΩ, Millipore) and diluted on the day of use. Iron solutions ($FeSO_4 \cdot xH_2O$) were prepared fresh on the day of use. Unless otherwise specified, all other chemicals were from Sigma Aldrich (Castle Hill, Sydney Australia).

2.1. Thioflavin t (ThT) time-resolved fluorescence

Stock solutions of NKB were diluted to 200 μM in either sodium phosphate buffer (NaP_i; 10 mM, 20 mM or 50 mM) or *N*-ethylmorpholine (n-EM; 10 mM) in a black-walled, clear bottom, sterile 96-well microplate (BMG Labtech) and incubated with 10 μM ThT for up to 48 h at 37 °C in a microplate reader (BMG FLUOROstar OPTIMA microplate reader). The plate was covered in clear sealing film, shaken for 5 s prior to data acquisition with excitation at 440 ± 5 nm and emission detected at 490 ± 10 nm through the bottom of the plate. For metal experiments Cu(II), Fe(II), Zn(II) or Ni(II) was added to NKB either prior to incubation or after ThT fluorescence had plateaued. The pH in the wells of the 96-well plate was not explicitly tested.

2.2. Electron microscopy

Fibrillar NKB was prepared under the same conditions as described above but in the absence of ThT. A few microliters of each sample was aliquoted onto a 300-mesh copper formvar grid (Proscitech, Australia) and left for 5 min; excess liquid was subsequently wicked off. 2% uranyl acetate replacement stain (Proscitech, Australia) was added for 10 s and excess wicked off. Water was subsequently added to grids for 5 min, wicked off and the grid dried for 24 hrs. Image acquisition was done using a Zeiss Merlin FEGSEM at 30 kV.

2.3. Nuclear magnetic resonance (NMR)

NMR spectra were acquired on a Bruker Avance 300 MHz spectrometer equipped with a 5 mm TXI probe and operated with Topspin 3.1 software (Bruker Biospin, Germany). One dimensional 1H spectra were acquired with either 256 or 64 scans over a spectral width of 11 ppm and 64 K complex data points. The spectra were processed in Topspin or in SpinWorks 4. (Marat, 2014) All spectra were calibrated to residual DMSO protons at $\delta = 2.82$ ppm.

2.4. Electron paramagnetic resonance (EPR)

Continuous wave X-band (~9.4 GHz) EPR spectra were collected on a Bruker EMX spectrometer. Samples were transferred to a 4 mm O.D. quartz EPR tube and frozen in liquid nitrogen. Temperature of the EPR cavity was controlled at 140 ± 5 K using nitrogen vapour. The power was 0.63 mW, the modulation frequency was 100 kHz and the modulation amplitude was 4.0 G.

3. Results and discussion

3.1. NKB rapidly forms amyloid fibrils

We initially used the amyloid specific dye Thioflavin T (ThT) to investigate the amyloid formation propensity of NKB. In 10 mM n-EM NKB rapidly forms ThT positive fibrils and the ThT fluorescence plateaus in about 40–60 min at 37 °C (Fig. 1A) suggesting the presence of mature fibrils. It is believed that aggregation of functional amyloids lacks a significant lag phase which limits the generation of toxic oligomeric species. Our results for NKB support this given the ThT fluorescence increases quickly suggesting a very short lag phase. Analysis of NKB fibrilization was also undertaken using the amyloid selective fluorescent probe TPP-TPE. (Kumar et al., 2017) Similarly to ThT, TPP-TPE appears to indicate NKB rapidly forms fibrils [see supporting information (SI) Fig. S1], and the growth in fluorescence intensity precedes the ThT fluorescence. TPP-TPE is thought to report early oligomeric species compared to ThT and in previous studies ThT fluorescence consistently lags that of TPP-TPE. (Kumar et al., 2017) NKB fibrillises at the same rate in 10 mM NaP_i as it does in nEM, but this rate decreases as the ionic strength increases; at 50 mM NaP_i, a concentration similar to the phosphate concentration in dense core vesicles, the time taken to fibrilise extends to ~300 min. This is in contrast to many proteins and peptides which fibrillise at a greater rate in increasing ionic strength, but is consistent with previous molecular modelling suggesting that NKB fibrillization slows as the phosphate concentration increases. (Carballo-Pacheco et al., 2015) A recent study showed that a decrease in phosphate concentration, occuring when the contents of a secretory vesicle are released into the extracellular environment, leads to disassembly of the neuropeptide β-endorphin. (Nespovitaya et al., 2016) In contrast, for NKB the amyloid form is maintained at the lower phosphate concentration.

To confirm that ThT itself was not influencing the amyloid formation NMR and electron microscopy (EM) were used to follow aggregation in the absence of any exogenous additive. The aromatic region of the NMR spectrum of NKB acquired within 10 min of dilution into

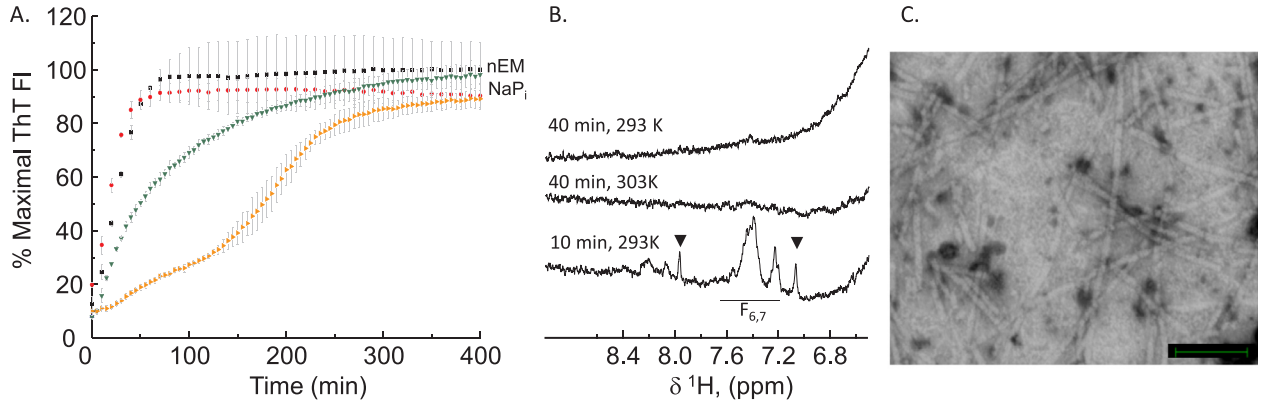

Fig. 1. Neurokinin B forms amyloid fibres. (A) Time resolved thioflavin (ThT) fluorescence in the presence of NKB in different conditions. NKB (235 μM) was prepared in 10 mM n-EM, pH 7.4 (■), 10 mM NaP_i, pH 7.2 (●), 20 mM NaP_i, pH 7.2 (▼) and 50 mM NaP_i, pH 7.4 (►). Error bars represent ± SD, n = 3. (B) NMR spectra (aromatic region) of NKB (230 μM) acquired within 10 min after dilution into 10 mM NaP_i, pH 7.4 (bottom trace) at 293 K, and after incubation in the spectrometer at 303 K for 40 min (middle trace) and after the temperature was returned to 293 K (top trace). Arrow heads signify His_3 imidazole C_2H (7.95 ppm) and C_4H (7.05 ppm), and $F_{6,7}$ denotes overlapping peaks from phenylalanine aromatic protons. (C) Electron micrograph of NKB fibrils obtained after incubation in 10 mM n-EM, pH 7.2. Scale bar is 0.1 μm.

10 mM n-EM shows peaks due to the phenylalanine aromatic side-chain protons (7.0–7.4 ppm) as well as histidine imidazole protons (C_4H 7.05 ppm, C_2H 7.95 ppm) (Fig. 1B, bottom trace). NKB was left in the NMR and the temperature increased from 298 K to 310 K, after 40 min spectra were acquired (Fig. 1B, middle trace). This spectrum shows only a broad peak around 7.3 ppm, suggesting that the apparent rotational correlation time has increased. The aliphatic region appeared complicated by the presence of peaks from non-deuterated DMSO, but loss of intensity of some peaks is observed suggesting aliphatic side-chains are affected by the fibril formation (Fig. S2) Decreasing the temperature to 298 K (Fig. 1B, top trace) appears to have no effect on the spectrum. The low signal-to-noise is due to the low concentration (230 μM) and the low number of scans acquired (ns = 256) to minimise the acquisition of spectra during the aggregation. An increase in the apparent rotational correlation time can be explained by the formation of high molecular weight species, consistent with amyloid formation, and the broadening of $Phe_{6,7}$ and His_3 side chain proton peaks suggests that these amino acids have lost their mobility – this may be a function of limited rotation due to their position in the interior of the amyloid. This is consistent with modelling studies showing that the phenylalanine amino acids in different monomers are interacting. (Carballo-Pacheco et al., 2015) Indeed, aromatic amino acids are often found between β-sheets in fibrils, as exemplified by amyloid-β, where phenylalanine amino acids in the core hydrophobic region (LVFFA) are critical for amyloid formation. (Cukalevski et al., 2012) The finding that $Phe_{6,7}$ and His_3 are involved in the core of the amyloid is supported by the fact that neither neurokinin A (lacking a Phe) and substance P (lacking a His) form fibrils under the conditions in which NKB does (Fig. S3A and B). We also note that the line broadening observed in the NMR may be partly due to microsecond to millisecond exchange processes given the fibril is likely in equilibrium with smaller NKB structure such as monomers and dimers. Lastly, EM analysis of NKB after dilution into 10 mM n-EM shows individual, unbranched structures of different lengths (Fig. 1C) consistent with fibrils and very similar to structures observed previously. (Maji et al., 2009) The fibrils were also investigated in solution using confocal microscopy and the results show the presence of clumps of fibrils interspersed with smaller individual structures (Fig. S3C). We predict that the larger clumps were dispersed when the sample was prepared for EM analysis.

3.2. Copper and nickel inhibit NKB amyloid formation.

We have previously shown that NKB binds copper(II) and nickel(II), with His_3 a critical residue for coordination. (Russino et al., 2013) To determine the effect of copper on *de novo* fibril formation we prepared apo-NKB and $[Cu^{II}(NKB)_2]$ in DMSO then diluted into 10 mM n-EM and used time-resolved ThT fluorescence to monitor fibril formation. An increase in ThT fluorescence over time indicated apo-NKB fibrillises as previously, but, in contrast, a minimal change in ThT fluorescence suggests $[Cu^{II}(NKB)_2]$ was unable to form extensive amyloid structures (Fig. 2A). The stoichiometry of copper and NKB under the fibrillization conditions is not known, but the inhibition of amyloid formation was dependent on the concentration of copper, increasing copper concentration from 0.5 to 1.5 equivalents Cu(II) resulted in a dose dependent reduction in the amount of ThT positive structures generated (Fig. S4A). The foregoing does not appear to be due to copper quenching of ThT fluorescence as previous studies have shown ThT fluorescence in the presence of copper and, furthermore, the absorption spectrum of ThT did not change in the presence of Cu(II) suggesting no interaction of the metal with ThT (Fig. S4B). (House et al., 2009) When visualised by electron microscopy, apo-NKB generated fibrillar structures (Fig. 2B) whereas almost no fibrils were observed in the NKB sample prepared in the presence of one equivalent of Cu(II). Copper coordination to other amyloidogenic proteins and peptides, including amyloid β, is thought to generate non-fibrillar, amorphous aggregates (House et al., 2009; Jiang et al., 2012; Mold et al., 2013), but no such aggregates were observed for copper-bound NKB. However, given the small size of NKB (11 amino acids), the formation of small oligomeric species that are not detectable by ThT or via EM cannot be ruled out.

Although copper can inhibit amyloid formation we wondered if the inhibition required high-affinity, specific binding to the peptide or whether any metal was sufficient. The other metal that is specifically bound to NKB is Ni(II) and the peptide is likely to encounter both Fe(II) and Zn(II) in the extracellular environment so we next determined if these metals could alter NKB fibrilization. Neither Zn(II) nor Fe(II) are known to coordinate to NKB with a physiologically relevant affinity. Using time-resolved ThT fluorescence Ni(II), like Cu(II), appears able to inhibit amyloid formation (Fig. 2C). In contrast, Fe(II) has little effect on the fibrilization although the overall amyloid content is reduced by ~25% which suggests that adventitious interactions do affect NKB fibril formation. Zn(II) was unable to inhibit the formation of NKB fibrils, but it did induce a very long lag phase (Fig. 2C). This suggests that Zn(II) can interact with NKB to some extent, most likely via His_3, to slow down but not inhibit fibrillogenesis. Whether zinc is still bound to the mature NKB fibrils is not known. Taken together this data can be used to imply that only specifically bound metals, namely Cu(II) and Ni(II), can completely inhibit fibril formation.

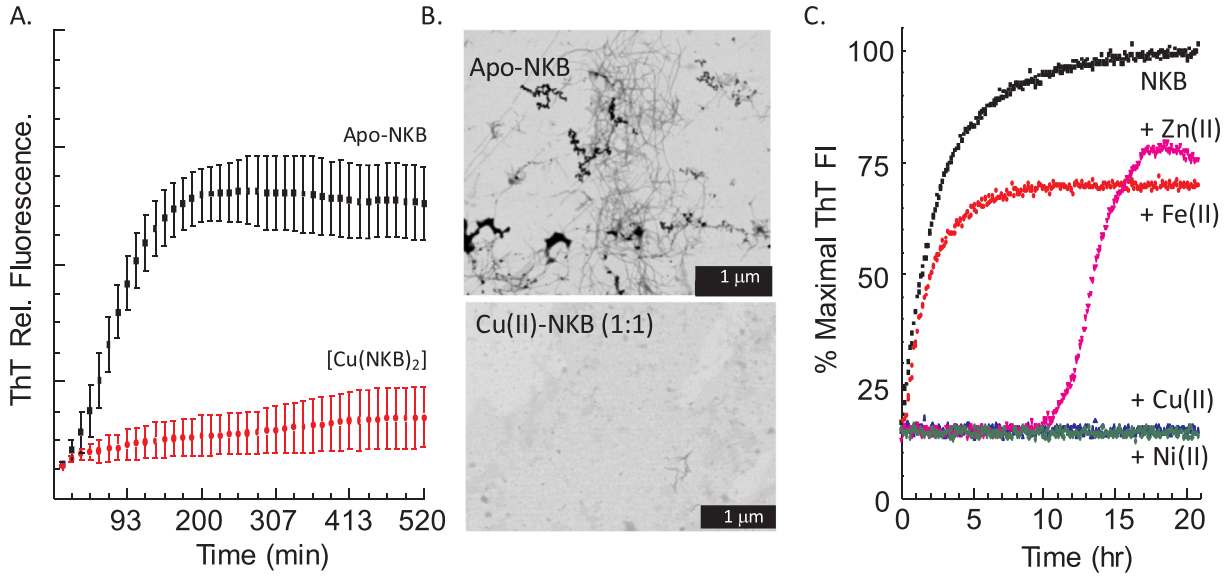

Fig. 2. Copper(II) and nickel(II) inhibit fibrillogenesis. (A) Time resolved ThT fluorescence in the presence of NKB (200 µM) in 10 mM n-EM, pH 7.8 in the absence of copper (Apo-NKB) or in the presence of 0.5 eq. Cu(II) ([$Cu^{II}(NKB)_2$].) Error bars are ± SD, n = 3. (B) Electron micrographs of samples obtained from apo-NKB in 10 mM n-EM, pH 7.8 (top) or from NKB incubated in the presence of 1 eq. Cu(II) (bottom). (C) Time resolved ThT fluorescence in the presence of NKB (200 µM, 10 mM NaP_i, pH 7.8) without metal (NKB) or with added Cu(II), Ni(II), Zn(II) or Fe(II). Each [metal] is 200 µM.

3.3. Cu(II) can disassemble preformed NKB fibrils

Amyloids are inherently stable molecules and resist degradation, but given Cu(II) can inhibit fibrillogenesis, we wanted to determine if the addition of copper to preformed fibrils contributed to disassembly. Firstly, one equivalent of Cu(II) was added to NKB after the peptide had formed ThT positive amyloids (Fig. 3A). Subsequently the addition of metal appeared to rapidly reduce fluorescence intensity. EM analysis of NKB fibrils that had been treated with copper showed no evidence of fibrillar structures suggesting that the metal was disassembling the fibres. To confirm that disassembly occurred because Cu(II) was able to coordinate NKB even when the peptide was involved in a fibril EPR was used. In EPR, unlike NMR, at low temperatures the spectral linewidths are not influenced by the aggregation state of the peptide and therefore the coordination environment of Cu(II) can be probed even when NKB is in a high molecular weight conformation. Initially, ThT positive fibrils were generated then one equivalent of Cu(II) was added to a sample in an EPR tube and immediately frozen in liquid nitrogen. This was considered the time 0 min sample. The EPR spectrum of this sample (Fig. 3B) shows a spectrum typical of axially symmetric Cu(II) ion ($g_{x,y} < g_z$), and plotting the g_z and A_z values on a Peisach-Blumberg plot suggests copper is in a 4 N or 3N1O coordination environment, i.e. it is bound to the peptide and not just aquated copper. (Peisach and Blumberg, 1974) The sample was removed from the spectrometer, allowed to thaw then left at room temperature for 30 min. After this time the sample was again frozen and the EPR spectrum acquired. This spectrum (Fig. 3B) has features identical to the time 0 min spectrum. Furthermore the g values at both time points are very close to those obtained from copper-bound NKB when in 10 mM n-EM/30 mM SDS. (Russino et al., 2013) This data suggests that copper is binding to NKB with the same coordination irrespective of whether the peptide is fibrillar or not. To confirm this we took the second differential of the time 0 min and 30 min spectra and focused on the $g_{x,y}$ region of the spectra (Fig. 3C). This region shows peaks lying on the main $g_{x,y}$ transition that are due to coupling between the electron on Cu^{2+} and the nuclear moment of a coordinated nitrogen atom (superhyperfine coupling, shf). The number of shf peaks in this region is identical in both the 0 min and 30 min samples confirming the same coordination in both samples. Furthermore, the 0 min and 30 min spectra are not only identical in the g values but also in the shf pattern to the second differential EPR spectrum of copper-bound NKB when in 10 mM n-EM/30 mM SDS, pH 7.4 (Fig. 3C). Under these conditions His_3 acts as an anchoring amino acid for copper coordination to the peptide and the similarity in the EPR spectra suggests that it is likely the case when copper binds to fibrillar NKB.

Along with copper(II), nickel(II) can bind to NKB and inhibit *de novo* fibril formation. The coordination of Ni(II) to NKB in results in the formation of a square-planar diamagnetic complex. (Russino et al., 2013) The diamagnetism means that NMR can be used to follow the effect of Ni(II) when added to preformed NKB fibrils. Firstly, the spectrum of apo-NKB was acquired after dilution into buffer (Fig. 4a) then the peptide was allowed to fibrillise and the NMR spectrum was collected (Fig. 4b). As per Fig. 1B this latter spectrum had no visible aromatic peaks due to aggregation-induced line broadening. We next added one equivalent Ni(II) and allowed the sample to incubate for 40 min prior to acquisition of the NMR spectrum. In contrast to the fibrillar apo-NKB spectrum, the NMR spectrum collected after the addition of Ni(II) had observable peaks (Fig. 4c). The spectrum does not change when the sample is left for a further 20 min (Fig. 4d). As in Fig. 1, these peaks are due to aromatic protons of phenylalanine and histidine amino acids, and the explanation for them reappearing is that Ni(II) has disassembled the NKB fibrils and the resulting complex has a rotational correlation time that allows protons to be observed by NMR. It is not clear what the complex is given that the pH of this experiment was *ca.* 7.4, and Ni(II) prefers a high pH to deprotonate amide nitrogens and promote coordination, but comparison of the Ni(II)-bound spectrum with that of apo-NKB (Fig. 4a) shows that the peaks that are most affected are those initially at 7.05 and 7.95 ppm, which we assign to the histidine imidazole C_4H and C_2H protons respectively (Fig. 4a and c, arrowed). We predict that the upfield movement of these peaks (to 6.98 ppm (C_4H) and 7.55 ppm (C_2H)) is due to coordination of Ni(II) to a nitrogen from the histidine imidazole group. (Tran et al., 2019) It is likely that under these conditions coordination of Ni(II) to the histidine is key to disassembly, which is consistent with the results from Cu(II) addition. This suggests that the nature of the metal is less critical, but rather its ability to coordinate to the histidine and disrupt the involvement of this residue in the amyloid fibre is important. Indeed, this is consistent with the results with Zn(II) – this metal does have some affinity for nitrogen donors, including imidazole nitrogens, but it is lower that that of Cu(II) and Ni(II) and hence Zn(II) can increase the

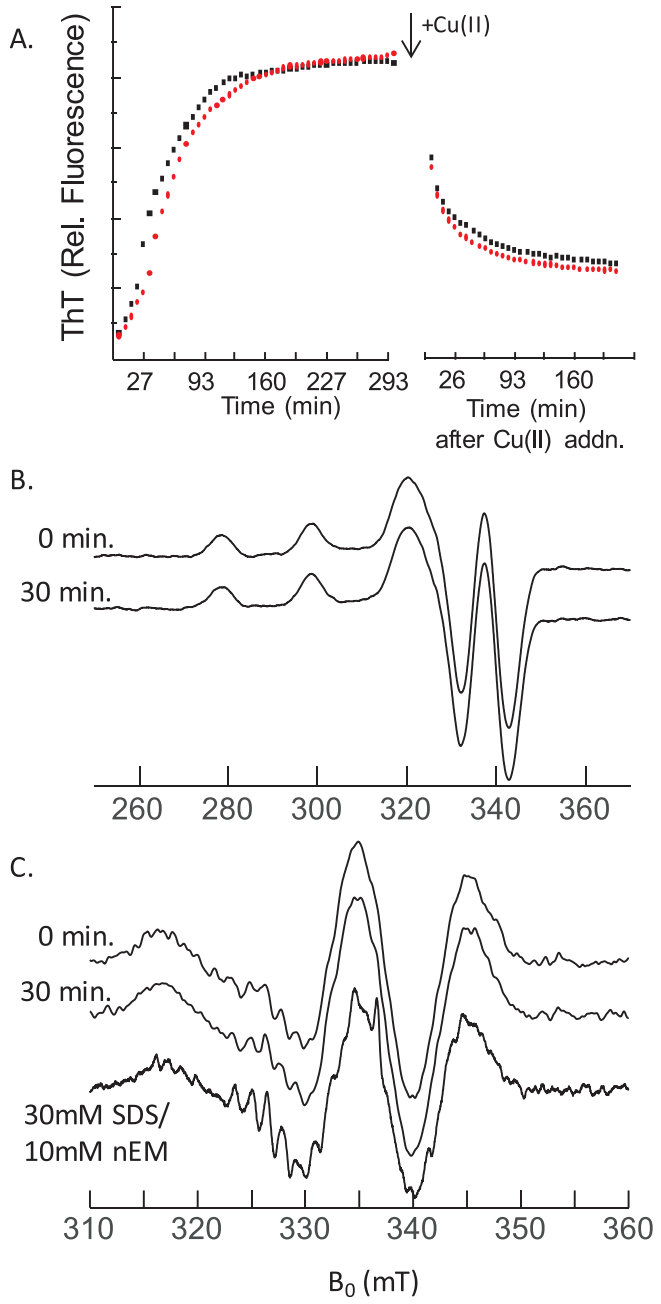

Fig. 3. Copper(II) disassembles NKB fibres. (A) Time resolved ThT fluorescence in the presence of apo-NKB (200 μM, 10 mM n-EM, pH 7.4) (left) and after the addition of 0.5 eq. Cu(II) (arrow signifies addition of Cu(II)). (B). First derivative X-band ($\nu \sim 9.4$ GHz) EPR spectra of NKB (250 μM, 10 mM n-EM, pH 7.6) acquired directly after addition of 1.0 eq. Cu(II) to NKB fibrils (0 min) and after the sample was incubated at room temperature for 30 min (30 min). (C) Second differential spectra of (B) with expansion of the region around $g_{x,y}$ compared to the same region of a spectrum of $[Cu^{II}(NKB)_2]$ in 10 mM n-EM/30 mM SDS, pH 7.4.

fibril lag time but not inhibit it completely (Fig. 3C), and contrasts with Fe(II) which usually prefers oxygen donor groups and does not inhibit fibril formation.

3.4. Histidine 3 in NKB is a key residue for fibril formation

The previous data suggested that the conformation of histidine 3 is important for the fibril structure and that metal coordination changes the conformation enough to induce fibril disassembly. To test the

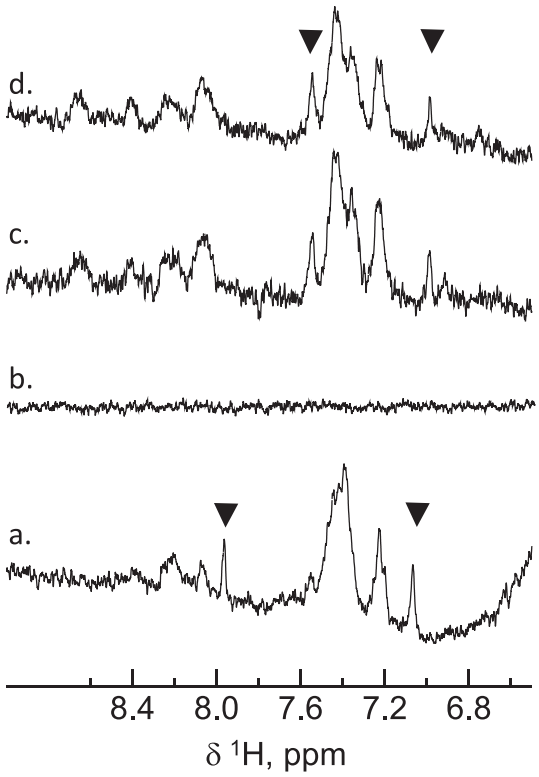

Fig. 4. Diamagnetic nickel(II) promotes NKB amyloid disassembly. The aromatic region of the NMR spectrum of apo-NKB (230 μM, 10 mM NaP_i, pH 7.4) has peaks due to His_3 and $Phe_{5,6}$ (a). The peaks broaden into the noise when the same sample was incubated at 37 °C for 40 min (b). After incubation for 20 min in the presence of 1.0 eq. Ni(II) the aromatic peaks return (c) and do not change after a further 40 min incubation (d). The arrow heads signify peaks tentatively assigned to C_2H and C_4H of the His_3 imidazole side-chain in apo-NKB (a) and after Ni(II) coordination (c).

importance of His_3 in the fibrillogenesis a mutant lacking this amino acid was prepared. This peptide, NKB(H_3T), did not form ThT positive amyloid structures (Fig. 5A) confirming the requirement for histidine to form an amyloid. The NMR data indicated that His_3, Phe_6 and Phe_7 are all involved in amyloid formation (Fig. 1B), which we speculate is via π-stacking interactions, and it is likely that loss of or disruption to His_3 does not allow these interactions to occur.

Given that His_3 appears critical for amyloid formation we wanted to determine if the pH was important, especially as the pH of the secretory granule is low (pH $<$ 6) and the granule contents (i.e. the peptide) are secreted into the extracellular environment (pH $>$ 7). The pKa of the imidazole group is ~ 6.5 and at pHs higher than this the histidine is a neutral and aromatic τ-tautomer and lower than this has a positively charged side chain. (Valery et al., 2015) Fig. 5B shows that at pH 7.4 and pH 5.6 NKB forms ThT positive fibrils, but at pH 5.6 the fluorescence intensity is lower suggesting the formation of fewer fibrils. The actual fibril formation may be due to the proportion of NKB that is in the uncharged state, and the proportion with the imidazolium side-chain does not fibrillise or NKB forms a structure at pH 5.6 that ThT cannot interact with as efficiently as to pH 7.4 fibrils. The latter appears more likely given, in the work of Maji et al. (2009), NKB was noted as forming amyloid at pH 5.5 having a structure not consistent with the common cross β -sheet structure, although we note that mannitol was included in those experiments which may have influenced the final structure. Furthermore, even in the protonated state the histidine imidazole ring is still able to participate in π–π stacking interactions which are reportedly more stable than interactions involving a neutral imidazole group. (Cauet et al., 2005, Liao et al., 2013) In any case, the addition of copper to NKB at pH 5.6 results in the rapid disassembly of

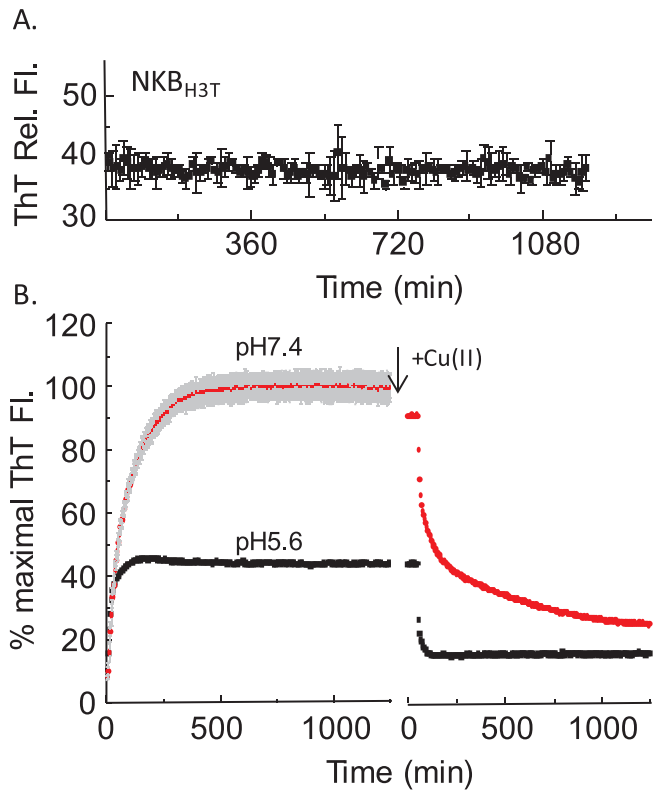

Fig. 5. His_3 is key for fibril formation. (A) Time resolved ThT fluorescence in the presence of the single point mutant NKB(H_3T) (200 μM, 10 mM n-EM, pH 7.4) shows no increase in fluorescence suggesting a lack of amyloid formation. (B) Time resolved ThT fluorescence in the presence of NKB (200 μM, 10 mM NaP_i) at pH 7.4 and pH 5.6. Fibril formation is limited at pH 5.6 compared to pH 7.4.

the fibril as it does at pH 7.4 (Fig. 5B).

4. Conclusions

This work demonstrates that release of NKB into a neutral pH, low phosphate environment such as that present in extracellular regions, is unlikely to cause disassembly of the NKB amyloid, but conversely these conditions will promote fibrillogenesis. This is counter to the idea that release of an amyloid from a secretory granule is sufficient to cause disassembly and formation of a functional conformation, although we predict dilution effects may contribute to some disassembly. (Maji et al., 2009) Our data suggests that in the bulk solution NKB amyloid will remain unless or until copper is present, whereupon the amyloid will be rapidly disassembled and the metal-bound peptide will activate the NK3 receptor. The complete lack of fibril formation when His_3 is missing suggests this residue is the molecular switch that controls fibrillogenesis. This can be explained by His_3 forming π–π stacking interactions with the phenylalanine side chains resulting in an extended conformation that promotes fibril formation. Indeed, histidine is known to form these interactions with aromatic amino acids, and is one way fibril formation is mediated in A β peptides. (Liao et al., 2013; Brannstrom et al., 2017) Aromatic-aromatic interactions have recently been predicted to help stabilise non-hydrogen-bonded β -strands in proteins and aromatic 'zippers' are thought to help stabilise inter-sheet packing in many amyloid fibrils. (Makin et al., 2005; Bemporad et al., 2006; Budyak et al., 2013) We previously identified aromatic clusters as being important for self-association of an echinoderm SALMFamide neuropeptide. (Otara et al., 2014) In the tachykinins, more than two aromatic residues are required, because neither NKA nor substance P form fibrils under the conditions that NKB does (Fig. S3A and B). Histidine-aromatic clusters that mediate large protein conformational changes have been identified in the peptide triptorelin (pEHWSY(D)WLRPG-NH_2) where the His_2 protonation state controls self-organisation of the peptide. (Valery et al., 2015) Rather than being limited to pH changes, we suggest that metals that coordinate histidine can disrupt a histidine-aromatic cluster by changing the peptide conformation around the histidine. The driving force is the thermodynamic stability of the histidine – cation (metal) interaction which is greater than that of the π–π interaction. (Liao et al., 2013) In NKB coordination of copper means histidine can no longer contribute to the aromatic cluster required for fibril stability and the amyloid disassembles (illustrated in Fig. S5). Cu(II) is particularly effective at modifying protein conformation because it can coordinate the histidine side chain along with back-bone amide nitrogens.

Physiologically, we postulate that when fibrillar NKB is released into areas that have a neutral pH (i.e. the synaptic or peri-synaptic region) copper is the 'key' that mediates the conformation of the peptide. It is established that copper is released from synaptic vesicles and can potentially reach micromolar concentrations in the synaptic space. (Kardos et al., 1989; Hopt et al., 2003) This copper is not bound to high-molecular weight molecules, and is able to interact with extracellular species such as receptors, neuropeptides and neurotransmitters. (Schlief et al., 2005; Gaier et al., 2013; Saito et al., 2019) NKB is highly expressed in anterior hypothalamic neurons, consistent with its influence on human reproductive health, and the hypothalamus, and anterior pituitary, are brain regions that are quite rich in copper. (Rance et al., 2010; Hare et al., 2012; Bonnemaison et al., 2016) Although this region is copper-rich due to the involvement of the metal in intracellular processes, copper is known to be released from synaptosomes derived from the median eminence suggesting that copper and NKB will co-exist extracellularly. We know that copper-bound NKB can activate the NK3 receptor, (Russino et al., 2013) and therefore the metal does not cause formation of aggregates but likely promotes monomeric or dimeric species capable of receptor activation. The Cu(II) induced disassembly of NKB fibrils to produce an active conformation is in stark contrast to the copper induced aggregation of several proteins implicated in neurodegenerative disorders, including α-synuclein associated with Parkinson's disease and A $\beta_{40/42}$ peptides. In these proteins copper promotes amorphous aggregates which are considered to have low toxicity but also little, if any, functionality.

The fate of copper once it has bound NKB and disassembled the amyloid is unclear, but receptor binding triggers endocytosis of the ligand/receptor complex and during endocytic processing we predict that copper is removed from NKB and either recycled or stored. (Christofides et al., 2018) How and where this occurs remains to be determined. This study deepens the place of copper in NKB function and suggests that NK3R activation is not just dependent on the presence or absence of the peptide in the extracellular space but is also dependent on copper and the conformational state of the peptide. Overall, this study expands our understanding of amyloid formation and disassembly and the role that metals can play in this process.

Declaration of Competing Interest

The authors declare that they have no known competing financial interests or personal relationships that could have appeared to influence the work reported in this paper

Acknowledgements

Dr Donald Thomas and the Mark Wainwright Analytical Centre, University of New South Wales, is thanked for assistance with EPR operation. Prof. Lawrence Berliner, University of Denver, is thanked for helpful EPR assistance and discussion.

Appendix A. Supplementary data

Experimental section, time resolved fluorescence using TPE-TPP, aliphatic regions of NMR spectra, ThT fluorescence of Neurokinin A and Substance P, confocal analysis of NKB fibrils, effect of copper concentration on inhibition of NKB amyloid formation, effect of copper on ThT absorption, schematic of copper disassembly of NKB fibrils. Supplementary data to this article can be found online at https://doi.org/10.1016/j.jsb.2019.09.011.

References

Bemporad, F., Calloni, G., Campioni, S., Plakoutsi, G., Taddei, N., Chiti, F., 2006. Sequence and structural determinants of amyloid fibril formation. Acc. Chem. Res. 39, 620–627.

Bonnemaison, M.L., Duffy, M.E., Mains, R.E., Vogt, S., Eipper, B.A., Ralle, M., 2016. Copper, zinc and calcium: imaging and quantification in anterior pituitary secretory granules. Metallomics 8, 1012–1022.

Brannstrom, K., Islam, T., Sandblad, L., Olofsson, A., 2017. The role of histidines in amyloid beta fibril assembly. FEBS Lett. 591, 1167–1175.

Budyak, I.L., Zhuravleva, A., Gierasch, L.M., 2013. The role of aromatic-aromatic interactions in strand-strand stabilization of beta-sheets. J. Mol. Biol. 425, 3522–3535.

Carballo-Pacheco, M., Ismail, A.E., Strodel, B., 2015. Oligomer formation of toxic and functional amyloid peptides studied with atomistic simulations. J. Phys. Chem. B 119, 9696–9705.

Cauet, E., Rooman, M., Wintjens, R., Lievin, J., Biot, C., 2005. Histidine-aromatic interactions in proteins and protein-ligand complexes: quantum chemical study of X-ray and model structures. J. Chem. Theory Comput. 1, 472–483.

Christofides, K., Menon, R., Jones, C.E., 2018. Endocytosis of G protein-coupled receptors and their ligands: is there a role in metal trafficking? Cell Biochem. Biophys. 76, 329–337.

Cukalevski, R., Boland, B., Frohm, B., Thulin, E., Walsh, D., Linse, S., 2012. Role of aromatic side chains in amyloid beta-protein aggregation. ACS Chem. Neurosci. 3, 1008–1016.

Dong, J., Canfield, J.M., Mehta, A.K., Shokes, J.E., Tian, B., Childers, W.S., Simmons, J.A., Mao, Z., Scott, R.A., Warncke, K., Lynn, D.G., 2007. Engineering metal ion coordination to regulate amyloid fibril assembly and toxicity. Proc. Natl. Acad. Sci. U.S.A. 104, 13313–13318.

Flashner, E., Raviv, U., Friedler, A., 2011. The effect of tachykinin neuropeptides on amyloid beta aggregation. Biochem. Biophys. Res. Commun. 407, 13–17.

Fowler, D.M., Koulov, A.V., Alory-Jost, C., Marks, M.S., Balch, W.E., Kelly, J.W., 2006. Functional amyloid formation within mammalian tissue. PLoS Biol. 4 e6.

Fowler, D.M., Koulov, A.V., Balch, W.E., Kelly, J.W., 2007. Functional amyloid–from bacteria to humans. Trends Biochem. Sci. 32, 217–224.

Gaier, E.D., Eipper, B.A., Mains, R.E., 2013. Copper signaling in the mammalian nervous system: synaptic effects. J. Neurosci. Res. 91, 2–19.

Gajewska, A., Zielinska-Gorska, M., Wolinska-Witort, E., Siawrys, G., Baran, M., Kotarba, G., Biernacka, K., 2016. Intracellular mechanisms involved in copper-gonadotropin-releasing hormone (Cu-GnRH) complex-induced cAMP/PKA signaling in female rat anterior pituitary cells in vitro. Brain Res. Bull. 120, 75–82.

Gul, A.S., Tran, K.K., Jones, C.E., 2018. Neurokinin B and serum albumin limit copper binding to mammalian gonadotropin releasing hormone. Biochem. Biophys. Res. Commun. 497, 1–6.

Hare, D.J., Lee, J.K., Beavis, A.D., van Gramberg, A., George, J., Adlard, P.A., Finkelstein, D.I., Doble, P.A., 2012. Three-dimensional atlas of iron, copper, and zinc in the mouse cerebrum and brainstem. Anal. Chem. 84, 3990–3997.

Hopt, A., Korte, S., Fink, H., Panne, U., Niessner, R., Jahn, R., Kretzchmar, H., Herms, J., 2003. Methods for studying synaptosomal copper release. J. Neurosci. Methods 128, 159–172.

House, E., Mold, M., Collingwood, J., Baldwin, A., Goodwin, S., Exley, C., 2009. Copper abolishes the beta-sheet secondary structure of preformed amyloid fibrils of amyloid-beta(42). J. Alzheimers. Dis. 18, 811–817.

Jacob, R.S., Das, S., Ghosh, S., Anoop, A., Jha, N.N., Khan, T., Singru, P., Kumar, A., Maji, S.K., 2016. Amyloid formation of growth hormone in presence of zinc: relevance to its storage in secretory granules. Sci. Rep. 6, 23370.

Jiang, D., Rauda, I., Han, S., Chen, S., Zhou, F., 2012. Aggregation pathways of the amyloid beta(1–42) peptide depend on its colloidal stability and ordered beta-sheet stacking. Langmuir 28, 12711–12721.

Kardos, J., Kovács, I., Hajós, F., Kálmán, M., Simonyi, M., 1989. Nerve endings from rat brain tissue release copper upon depolarization. A possible role in regulating neuronal excitability. Neurosci. Lett. 103, 139–144.

Kawahara, M., Koyama, H., Nagata, T., Sadakane, Y., 2011. Zinc, copper, and carnosine attenuate neurotoxicity of prion fragment PrP106-126. Metallomics 3, 726–734.

Knowles, T.P., Vendruscolo, M., Dobson, C.M., 2014. The amyloid state and its association with protein misfolding diseases. Nat. Rev. Mol. Cell. Biol. 15, 384–396.

Kumar, M., Hong, Y., Thorn, D.C., Ecroyd, H., Carver, J.A., 2017. Monitoring early-stage protein aggregation by an aggregation-induced emission fluorogen. Anal. Chem. 89, 9322–9329.

Liao, S.M., Du, Q.S., Meng, J.Z., Pang, Z.W., Huang, R.B., 2013. The multiple roles of histidine in protein interactions. Chem. Cent. J. 7, 44.

Maji, S.K., Perrin, M.H., Sawaya, M.R., Jessberger, S., Vadodaria, K., Rissman, R.A., Singru, P.S., Nilsson, K.P., Simon, R., Schubert, D., Eisenberg, D., Rivier, J., Sawchenko, P., Vale, W., Riek, R., 2009. Functional amyloids as natural storage of peptide hormones in pituitary secretory granules. Science 325, 328–332.

Makin, O.S., Atkins, E., Sikorski, P., Johansson, J., Serpell, L.C., 2005. Molecular basis for amyloid fibril formation and stability. Proc. Natl. Acad. Sci. U.S.A. 102, 315–320.

Marat, K., 2014. Spinworks, 4.1.0. University of Manitoba, Canada.

Mold, M., Ouro-Gnao, L., Wieckowski, B.M., Exley, C., 2013. Copper prevents amyloid-beta(1–42) from forming amyloid fibrils under near-physiological conditions in vitro. Sci. Rep. 3, 1256.

Nassel, D.R., 2009. Neuropeptide signaling near and far: how localized and timed is the action of neuropeptides in brain circuits? Invert. Neurosci. 9, 57–75.

Nespovitaya, N., Gath, J., Barylyuk, K., Seuring, C., Meier, B.H., Riek, R., 2016. Dynamic assembly and disassembly of functional beta-endorphin amyloid fibrils. J. Am. Chem. Soc. 138, 846–856.

Otara, C.B., Jones, C.E., Younan, N.D., Viles, J.H., Elphick, M.R., 2014. Structural analysis of the starfish SALMFamide neuropeptides S1 and S2: the N-terminal region of S2 facilitates self-association. Biochim. Biophys. Acta Proteins Proteom. 1844, 358–365.

Peisach, J., Blumberg, W.E., 1974. Structural implications derived from the analysis of electron paramagnetic resonance spectra of natural and artificial copper proteins. Arch. Biochem. Biophys. 165, 691–708.

Rance, N.E., Krajewski, S.J., Smith, M.A., Cholanian, M., Dacks, P.A., 2010. Neurokinin B and the hypothalamic regulation of reproduction. Brain Res. 1364, 116–128.

Riek, R., Eisenberg, D.S., 2016. The activities of amyloids from a structural perspective. Nature 539, 227–235.

Russino, D., McDonald, E., Hejazi, L., Hanson, G.R., Jones, C.E., 2013. The tachykinin peptide neurokinin B binds copper forming an unusual [CuII(NKB)] complex and inhibits copper uptake into 1321N1 astrocytoma cells. ACS Chem. Neurosci. 4, 1371–1381.

Saito, K., Watanabe, K., Yanaoka, R., Kageyama, L., Miura, T., 2019. Potential role of serotonin as a biological reductant associated with copper transportation. J. Inorg. Biochem. 199 110770.

Schlief, M.L., Craig, A.M., Gitlin, J.D., 2005. NMDA receptor activation mediates copper homeostasis in hippocampal neurons. J. Neurosci. 25, 239–246.

Shahzad, R., Jones, M.R., Viles, J.H., Jones, C.E., 2016. Endocytosis of the tachykinin neuropeptide, neurokinin B, in astrocytes and its role in cellular copper uptake. J. Inorg. Biochem. 162, 319–325.

Tayeb-Fligelman, E., Tabachnikov, O., Moshe, A., Goldshmidt-Tran, O., Sawaya, M.R., Coquelle, N., Colletier, J.P., Landau, M., 2017. The cytotoxic Staphylococcus aureus PSMalpha3 reveals a cross-alpha amyloid-like fibril. Science 355, 831–833.

Topaloglu, A.K., Reimann, F., Guclu, M., Yalin, A.S., Kotan, L.D., Porter, K.M., Serin, A., Mungan, N.O., Cook, J.R., Ozbek, M.N., Imamoglu, S., Akalin, N.S., Yuksel, B., O'Rahilly, S., Semple, R.K., 2009. TAC3 and TACR3 mutations in familial hypogonadotropic hypogonadism reveal a key role for Neurokinin B in the central control of reproduction. Nat. Genet. 41, 354–358.

Tran, K.K., Jayawardena, B.M., Elphick, M.R., Jones, C.E., 2019. A gonadotropin-releasing hormone type neuropeptide with a high affinity binding site for copper(II) and nickel(II). Metallomics 11, 404–414.

Valery, C., Deville-Foillard, S., Lefebvre, C., Taberner, N., Legrand, P., Meneau, F., Meriadec, C., Delvaux, C., Bizien, T., Kasotakis, E., Lopez-Iglesias, C., Gall, A., Bressanelli, S., Le Du, M.H., Paternostre, M., Artzner, F., 2015. Atomic view of the histidine environment stabilizing higher-pH conformations of pH-dependent proteins. Nat. Commun. 6, 7771.

Yankner, B.A., Duffy, L.K., Kirschner, D.A., 1990. Neurotrophic and neurotoxic effects of amyloid beta protein: reversal by tachykinin neuropeptides. Science 250, 279–282.